Model for eukaryotic tail-anchored protein binding based on the structure of Get3

Christian J. M. Suloway, Justin W. Chartron, Ma'ayan Zaslaver, and William M. Clemons, Jr.[1]

Division of Chemistry and Chemical Engineering, California Institute of Technology, 1200 East California Boulevard, Pasadena, CA 91125

Communicated by Douglas C. Rees, California Institute of Technology, Pasadena, CA, July 8, 2009 (received for review June 24, 2009)

The Get3 ATPase directs the delivery of tail-anchored (TA) proteins to the endoplasmic reticulum (ER). TA-proteins are characterized by having a single transmembrane helix (TM) at their extreme C terminus and include many essential proteins, such as SNAREs, apoptosis factors, and protein translocation components. These proteins cannot follow the SRP-dependent co-translational pathway that typifies most integral membrane proteins; instead, post-translationally, these proteins are recognized and bound by Get3 then delivered to the ER in the ATP dependent Get pathway. To elucidate a molecular mechanism for TA protein binding by Get3 we have determined three crystal structures in apo and ADP forms from *Saccharomyces cerevisae* (*Sc*Get3-apo) and *Aspergillus fumigatus* (*Af*Get3-apo and *Af*Get3-ADP). Using structural information, we generated mutants to confirm important interfaces and essential residues. These results point to a model of how Get3 couples ATP hydrolysis to the binding and release of TA-proteins.

ArsA | crystallography | Deviant Walker A | Get pathway | protein transport

Tail-anchored (TA) proteins represent a large and diverse class of integral membrane proteins that are found in all organisms. These include numerous types of proteins, such as SNAREs, apoptosis factors, and protein translocation components. TA proteins are characterized by having a single transmembrane helix (TM) at their extreme C terminus. Due to this topological constraint, these proteins are not able to follow the SRP-dependent co-translational pathway that typifies most integral membrane proteins. Instead, these proteins must find their correct membrane for insertion post-translationally (reviewed in refs. 1 and 2).

The ATPase Get3 was the first protein identified directly involved in TA targeting and is part of the Get pathway (now known as Guided Entry of Tail-anchored proteins) that also contains the ER membrane proteins Get1/2 and the putative ribosome receptor proteins Get4/5 (3–7). Multiple studies have shown that Get3 binds directly to the hydrophobic tail-anchors and, in conjunction with ribosome and endoplasmic reticulum (ER) factors, utilizes an ATP cycle to bind and then release TA proteins at the ER membrane.

Get3 was originally annotated Asna-1/Arr4p due to its apparent homology (≈25% identity) to the bacterial arsenite transporter component ArsA (8). Get3 homologues had been implicated in a diverse set of functions now presumed to be linked to the correct localizations of TA proteins (9–12). Get3 is a protein-targeting factor, analogous to the signal recognition particle (SRP), and, similar to SRP components (13), is not essential for viability in yeast; however, the cells are sensitive to a variety of stresses such as heat and metals (14).

Get3 contains a nucleotide hydrolase domain (NHD) that resembles the G-type hydrolases characterized by Ras [for review see (15)]. These proteins all have the completely conserved 'P-loop' that recognize the α- and β-phosphate in both NDP and NTP states. Other features of G-type hydrolases are Switch I (A') and Switch II (Walker B) loops that undergo dramatic rearrangements coupling structural changes to the presence of the γ-phosphate. In these proteins, catalysis is stimulated by a positively charged residue that stabilizes negative charge on the phosphates and a residue that positions a catalytic water for nucleophilic attack.

Get3, like ArsA and the nitrogenase iron protein (NifH), belongs to a special class of ATPases that contain a 'deviant' Walker A motif which is a P-loop with an additional invariant lysine (G**K**GGVGKT in Get3) (16). This is a rare motif, found in only two other yeast proteins [including a putative Fe-protein homologue (17)]. A basic model for the deviant P-loop ATP hydrolysis cycle can be inferred by the structure of a NifH dimer bound to ADP·AlF_4^- and its partner the MoFe protein (18). The ADP and apo forms of NifH are in an open conformation that is inactive for ATP hydrolysis (19). Binding of the MoFe protein, along with ATP, causes a large rotational and translational shift of the two NifH monomers that brings the deviant P-loop lysine from the opposing monomer into a position to stabilize the build up of negative charge on the phosphates. This is analogous to the mechanism in Ras where an Arg-finger from a GAP stimulates hydrolysis of ATP leading to Ras inactivation (20, 21). This interface shift demonstrates how ATP can modulate dramatic structural changes. Critical to all of this, the rearrangements are stabilized by binding of the MoFe protein (18). In the case of ArsA, without its partner ArsB bound, no states are found in which both NHD bind the same nucleotide and it is reasonable to speculate that in a true ATP state a dramatic conformational change must occur as well (22, 23).

There are no mechanistic studies detailing how Get3 performs its important targeting function and a molecular level understanding requires structural information. Here we present three crystal structures of Get3/TRC40, a monomeric apo form from *Saccharomyces cerevisae* (*Sc*Get3) and dimeric apo and hexameric ADP-bound forms from the thermophilic opportunistic human pathogen *Aspergillus fumigatus* (*Af*Get3 and *Af*Get3-ADP). Based on the structures, we probed functional interfaces and essential residues by phenotypic rescue. Our results allow us to define a model of how Get3 couples ATP hydrolysis to the binding and release of TA-proteins. More broadly, this work supports a mechanism for a special class of ATPases.

Results

Crystallization of Get3. We purified *Sc*Get3 and *Af*Get3 from constructs expressed in *E. coli* using Ni-affinity and size exclusion chromatography under reducing conditions. The majority of the protein eluted as a dimer from both constructs and this was used in crystallization trials. The *Af*Get3-ADP crystals diffracted to 3.2-Å resolution in the space group $P2_12_12_1$ with a hexamer in

Author contributions: C.J.M.S. and W.M.C. designed research; C.J.M.S. performed research; C.J.M.S. and M.Z. contributed new reagents/analytic tools; C.J.M.S., J.W.C., and W.M.C. analyzed data; and C.J.M.S., J.W.C., and W.M.C. wrote the paper.

The authors declare no conflict of interest.

Data deposition: The atomic coordinates and structure factors have been deposited in the RCSB Protein Data Bank, www.pdb.org (PDB ID codes 31BG for *Af*Get3-ADP and 31DQ for *Sc*Get3).

[1]To whom correspondence should be addressed. Email: clemons@caltech.edu.

This article contains supporting information online at www.pnas.org/cgi/content/full/0907522106/DCSupplemental.

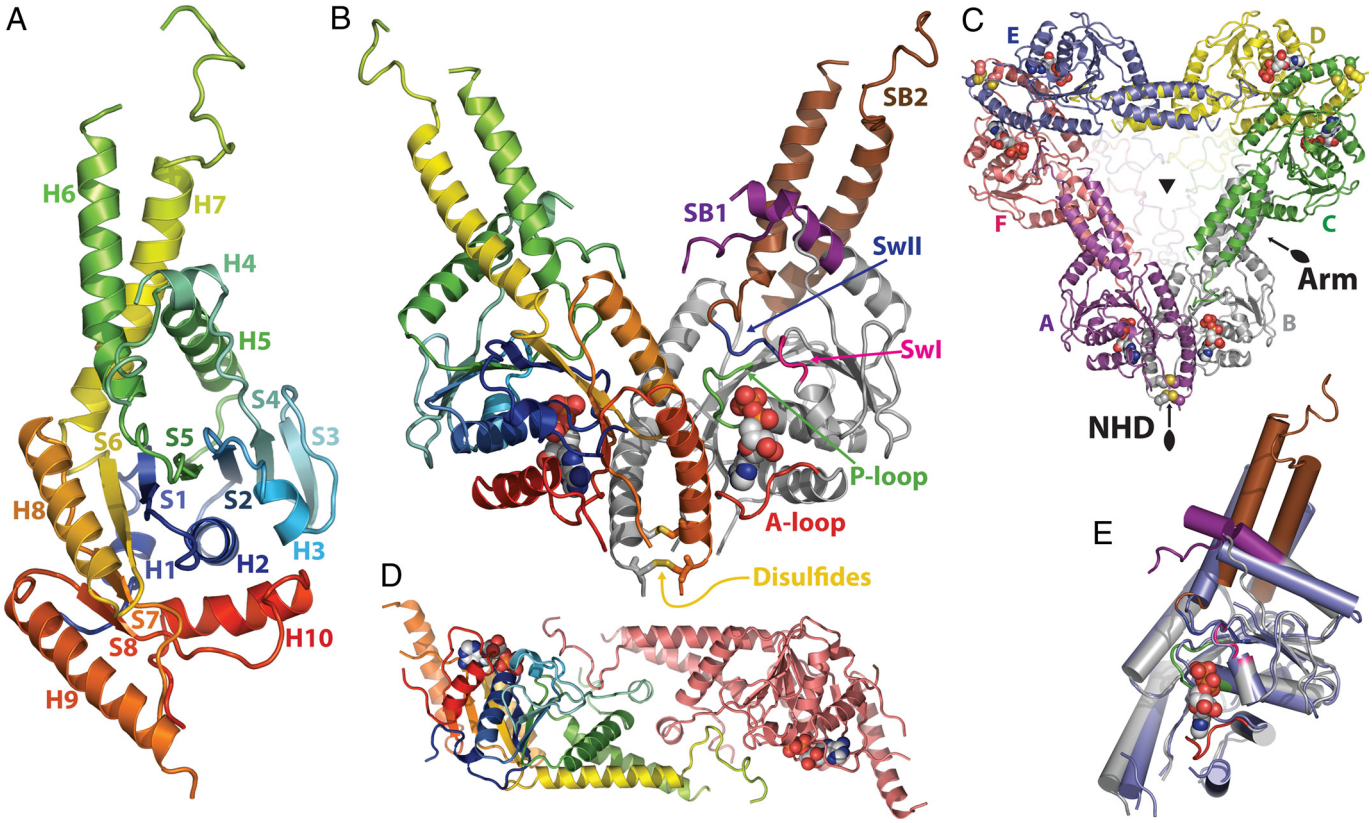

Fig. 1. Structures of Get3. (*A*) An *Af*Get3-ADP monomer with secondary structure elements numbered as in Fig. S1. (*B*) The NHD dimer of the *Af*Get3-ADP hexamer. One monomer is color ramped from N- (blue) to C- (red) and the other is colored relative to motifs described in the text: P-loop (green), Switch I (magenta), Switch II (blue), A-loop (red), SB1 (purple), and SB2 (brown). (*C*) The *Af*Get3-ADP hexamer of the asymmetric unit colored by monomers. Dimer interfaces and subunits are labeled. The 3-fold is indicated by a triangle and 2-folds are indicated by an oval. The modeled residues from SB1 of each monomer are transparent. Nucleotides and bridging disulfides are shown as spheres. (*D*) The arm dimer of the *Af*Get3-ADP hexamer. One monomer is color ramped as in *A* and the other is colored salmon. (*E*) The *Sc*Get3 model colored purple and overlayed with an *Af*Get3-ADP monomer colored and oriented as in *B*.

the asymmetric unit. A seleno-methionine data set was collected to 4.5-Å resolution and phases were solved by multiwavelength anomalous dispersion and extended to 3.2-Å resolution using the 6-fold noncrystallographic symmetry. The final refined structure contained 292 of 348 residues with a Free-R factor of 25.1% (Fig. 1*C* and Fig. S1). The two Apo forms of Get3 were solved using molecular replacement of a truncated *Af*Get3-ADP monomer. The *Sc*Get3-apo crystal form diffracted to 3.7-Å resolution in the space group H32 and contained a monomer in the asymmetric unit. The final model contained 260 of 369 residues and refined to a Free-R factor of 33.5% (Fig. S2 *A* and *B*). The *Af*Get3-apo crystal form diffracted to 7.5-Å resolution in the space group $P4_232$ and contained a dimer in the asymmetric unit that we did not refine due to the low resolution (Fig. S2*D*). Crystallographic statistics are provided in Table S1.

Description of a Get3 Monomer. The structure of a monomer of Get3 is a mixed alpha-beta fold containing a "P-loop" type NHD with two α-helical loops that extend outward from the structure, here designated substrate binding loop 1 (SB1) and 2 (SB2) (Fig. 1 *A* and *B*). The Get3 NHD fold falls into a more specific structural class [defined by SCOP (24)] that includes ArsA (25), GTPase domains of the signal recognition particle (SRP) (26), and SRP receptor (27) along with NifH (28). Get3 is the only eukaryotic example in this class that utilizes ATP.

The Three Crystal Forms of Get3. The *Af*-ADP crystal form contains a hexamer in the asymmetric unit (Fig. 1*C*) with 3-fold symmetry in which the monomer can be assembled into two potential dimers formed by either SB1/2 (arm dimer) or by the interface between the NHD (Fig. 1 *B* and *D*). Although the arm dimer contains a more extensive interface, 1758Å^2 versus 1263Å^2 calculated by PISA (29), we believe that the NHD dimer is the most relevant to TA-protein binding and contains two disulfides formed across the interface by a conserved pair of cysteines (Fig. 1*B*).

The *Sc*-apo crystal form contains a monomer in the asymmetric unit (Fig. 1*E* and Fig. S2*A*), and there is no apparent NHD dimer interface despite the protein purifying as a dimer. The crystals are stabilized by the coordination of a zinc by Cys-285/Cys-288 and the His-tag which also coordinates a second metal at the crystallographic three fold in a square-planar geometry (Fig. S2*A*). The *Af*Get3-apo contains two copies in the asymmetric unit in an orientation similar to the NHD dimer, although rotated so that the SB1 and SB2 regions of the two monomers are slightly closer (Fig. S2*E*). Both Apo crystal forms contain symmetry related interfaces similar to the arm dimer (Figs. S2*C* and S3*F*).

Monomers in each of the three crystal forms show slight variations in SB1/2 demonstrating the general mobility of these regions (Fig. 1*E* and Fig. S2*F*). These loops in the hexamer are stabilized by a series of hydrophobic interactions in a highly flexible region that perhaps explains the difficulty in obtaining high-resolution crystals. SB1 and SB2 contain disordered regions in all of the crystal forms. The missing residues of SB1 have been modeled into the *Af*Get3-ADP hexamer to demonstrate the amount of disordered protein that could not be built (Fig. 1*C*).

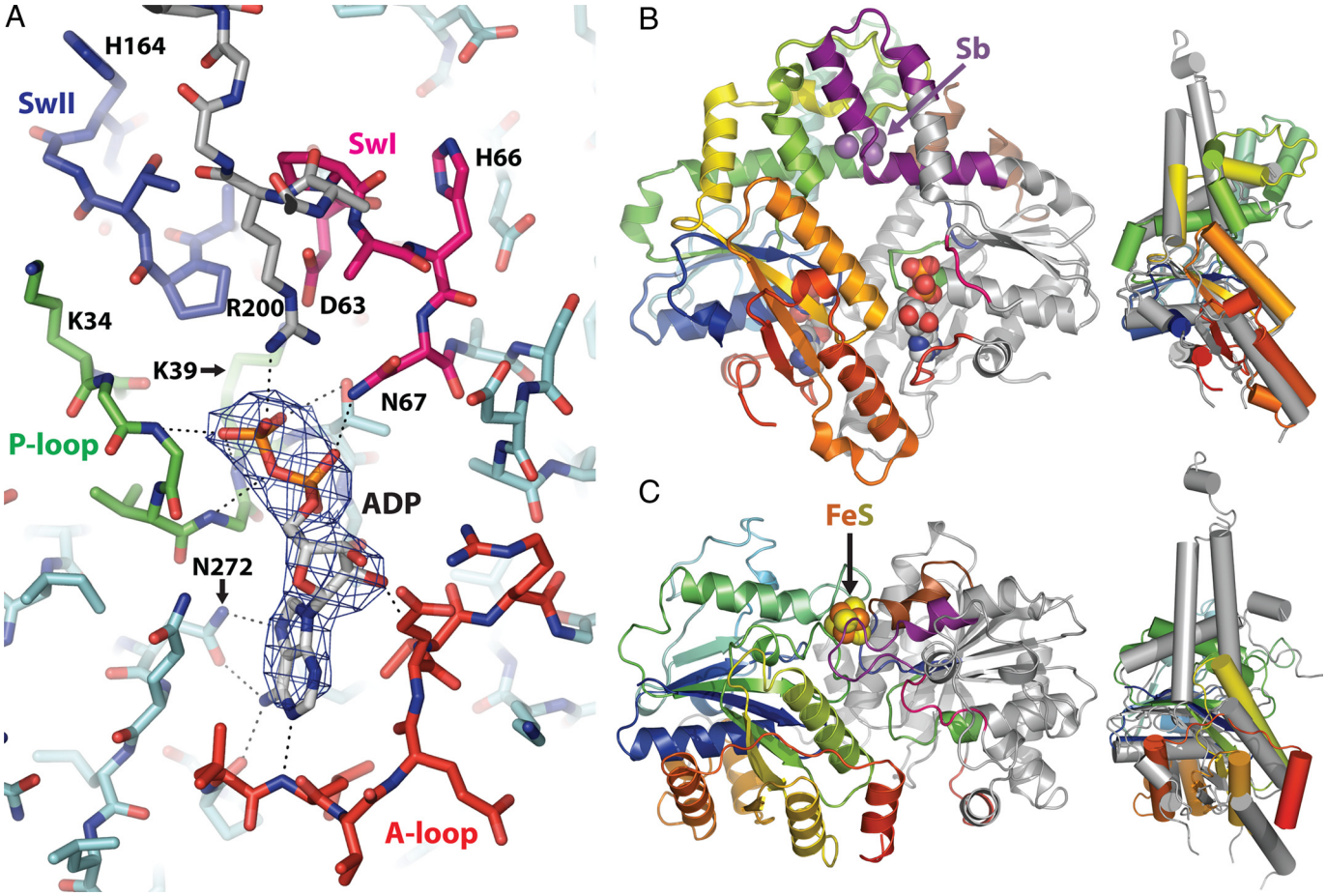

Fig. 2. The nucleotide-binding pocket and comparison of Get3 to other hydrolases. (*A*) The nucleotide-binding pocket of *Af*Get3-ADP with residues shown as sticks. Density is a 2Fo-Fc omit-map contoured at 1.5σ. (*B*) A ribbons diagram of the ADP form of *Ec*ArsA (1f48) with ADP, Mg^{2+} (green) and coordinated Sb (purple) as spheres. (*C*) A ribbon diagram of the apo form of NifH (2nip) with the Fe/S cluster (orange/yellow) as spheres. To the right in *B* and *C* are overlays of monomers the *Af*Get3-ADP monomer (gray) on the respective left subunit. Important residues and motifs are labeled. All residues in nucleotide binding motifs are colored as in 1*B*.

Nucleotide Binding. The Get3 nucleotide-binding pocket contains all of the features generally found in G-type hydrolases. The completely conserved Asn in S7 (*Sc*/*Af*272) forms hydrogen-bonds that specifically select for adenine. Additional interactions with the A-loop complete adenosine recognition (Fig. 2*A*). The P-loop, as is typical, makes extensive contacts to the α- and β-phosphate; however, the second lysine, completely conserved in P-loops, is in an orientation that points away from the β-phosphate. This is caused by an interaction in the arm dimer that leads to an Arg from SB2 (*Af*200) moving into the active site occupying a similar position near where one would expect Mg^{2+} to be bound (Fig. 2*A*). It is clear that *Af*R200 displaces the Mg^{2+} and generally disrupts the interactions of Switch I and II. Based on the resolution, we cannot be certain that there is no Mg^{2+}; however, if present it would be in a unique position. *Af*R200 forms a salt bridge to the β-phosphate; but it is not conserved making the extent of these interactions surprising.

Comparison to ArsA and NifH. Despite distinct functions, Get3 shares a similar topology to ArsA with an RMSD of 1.9Å in their NHD (Fig. 2*B*) (PDBID 1f48) (25). In contrast to Get3, ArsA SB1/2 bend in across the NHD dimer interface forming a coordination site for heavy metals (Fig. 2*A*); however, these coordinating residues are not conserved in Get3. It is thought that motions of these loops are coupled to ATP hydrolysis regulating metal release via the Switch II motif (22). The dimer interface is very similar to Get3 except that the interface is rotated moving the P-loop from 9.1-Å (G17/G336) separation in ArsA to 14.1 Å (*Af*G35) in Get3. An early homology model of Get3, based on ArsA, predicted the occurrence of the disulfide bridges between the subunits at the dimer interface. Based on the model they found that mutation of the two cysteines in Get3 was unable to rescue a metal sensitivity phenotype in a Get3 knockout (30). ArsA is a pseudodimer with a disordered linker peptide between the two subunits that may be required to stabilize the dimer interface.

The best understood deviant P-loop protein is NifH as its structure has been solved in Apo, ADP, and ADP·AlF_4^- forms. The structure closest to *Af*Get3-ADP is the NifH-Apo form (19) and the NHD domains have an RMSD of 2.78 Å. As noted, ATP stimulates a large conformational shift that moves the deviant P-loop (*A. vinelandii* NifH G11) from 10.1 Å to 4.0 Å apart. To move the Get3 dimer into a similar orientation would require an extensive conformational change across the dimer interface.

Tail-Anchor Binding Pocket. In a search for the TA-protein binding pocket, the positions of SB1 and SB2 are clearly provocative. We analyzed the NHD dimer by displaying conserved and hydrophobic residues on a molecular accessibility surface (Fig. 3). The interface, formed by the NHD dimers, is highly conserved, as is expected for a common fold (Fig. 3*A*). The other concentration of conserved residues is found at the base and groove formed by

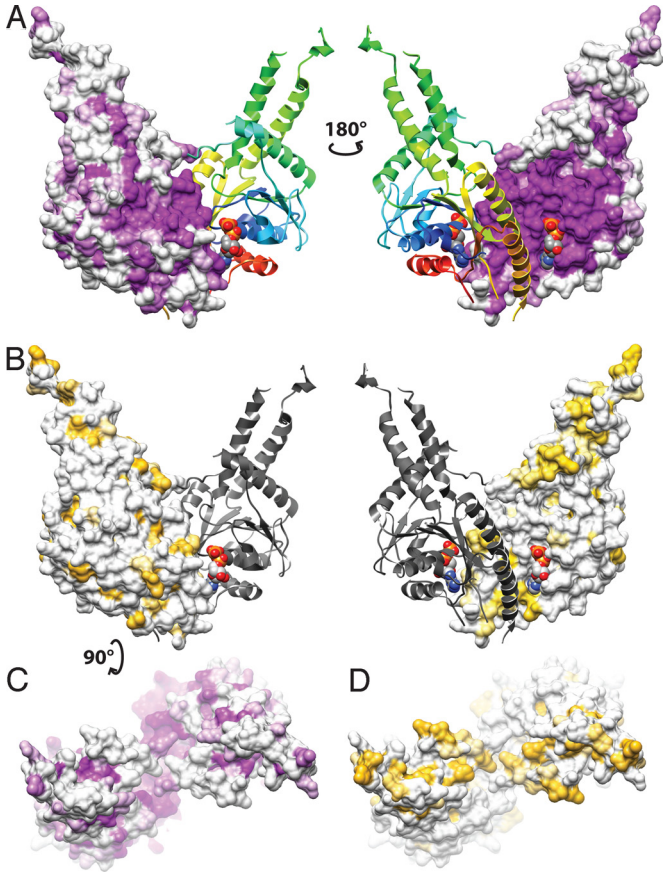

Fig. 3. Conserved and hydrophobic surfaces. (*A*) Front and back views showing one monomer as a ribbon colored as in 1*A* and the other as an accessible surface showing conservation colored as a gradient from 100% (purple) to 50% conserved (gray). Conservation is based on the Get3 alignment from Fig. S1 (*B*) Similar to *A* showing hydrophobicity based on the Kyte and Doolittle scale with most hydrophobic in dark yellow. (*C*) Conserved surface viewed from the top. (*D*) Hydrophobic surface viewed from the top.

SB1/SB2 (Fig. 3*C*). The overall alignment of SB1/SB2 is difficult; however, there is general conservation of hydrophobic residues and glycines (Fig. S1). Additionally, SB1 contains a disordered stretch that could also provide surface area in this region. The only hydrophobic patch on the surface of the dimer is that formed between SB1 and SB2 (Fig. 3 *B* and *D*). This putative TA-binding region would be analogous to the location of the metal binding sites of ArsA or the Fe-S cluster in NifH (Fig. 2 *B* and *C*) and one presumes that changes in the ATP binding pocket would be transmitted to this region.

Phenotypic Rescue. To probe the functional parts of Get3 we chose a series of mutants based on surface conservation or putative function and tested for their ability to rescue known knockout phenotypes (30). The knockout (Δ*get3*) showed no obvious impairment on synthetic complete media at 30C but was unable to fully rescue on media containing Cu^{2+} or hydroxyurea or growth at elevated temperature. Replacing the Get3 gene on a plasmid (*GET3*) with the wild-type promoter rescued the Δ*get3* growth to near wild-type levels. We also inserted the *Af*Get3 gene on the same plasmid and this also rescued the yeast knockout demonstrating that functional aspects of the protein are conserved across species (Fig. 4*A* and Fig. S3). In all, we generated 69 *Sc* mutants and two *Af* mutants and scored their general loss-of-function (LOF) phenotype as strong, moderate,

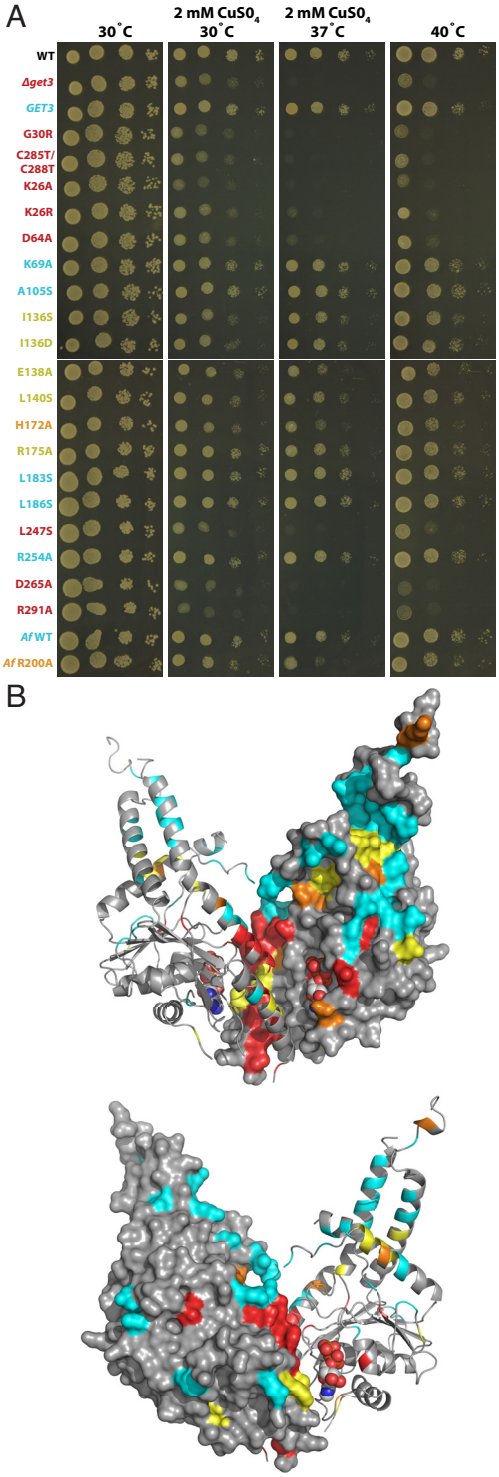

Fig. 4. Phenotypic rescue of various Get3 mutants. (*A*) Spot plate assays of various yeast mutants on a plasmid with a wild-type promoter screened on SC-Ura plates at 30C and 40C and supplemented with 2 mM $CuSO_4$ at both 30C and 37C. Δ*get3* is the knockout transformed with a plasmid containing only the promoter. Mutants based on yeast numbering are indicated colored relative to their phenotype: strong (red), moderate (orange), weak (yellow), and none (cyan). (*B*) Two views with one monomer as accessible surface and the other in ribbon colored according to phenotype as in *A*.

weak or none (Fig. 4*A* and *B*, data for all mutants in Fig. S3 and Table S2).

In agreement with previous results, a mutation in either the

P-loop (*Sc*G30R or *Af*G38R) or the pair of Cys that form the disulfide bridges (C285T/C288T) had strong LOF phenotypes (Fig. 4*A*) (3, 30). The G30R mutation is thought to disrupt ATP binding. The effect of the Cys mutants is less clear. Presumably, this interface is somewhat unstable and requires the disulfides to stabilize the dimer, similar to the linked dimer of ArsA. As the cytoplasm is a reducing environment, it would be curious that the disulfides could form in vivo; however, we included reducing agent in all of our buffers and the disulfides formed in that context. Another possibility is that these residues coordinate a metal or are regulated by a redox pathway (30) as the reduced form in the *Sc*Get3-apo crystals is a monomer and coordinates a zinc (Fig. S2 *A* and *B*).

The largest cluster of LOF mutants occurs at the NHD dimer interface found mostly on H8 and H9. The interface is a mixture of hydrophobic and charged groups that would be intimately involved in a re-arrangement of the dimer (Fig. S4*B*, Figs. S1 and S4*A*). Only a few of the conserved surface mutations that did not make contacts in this crystal form conferred LOF phenotypes (R75A, D265A, and Y338A) and probably do not affect the conformational changes in substrate binding (Fig. S4*B*). It is possible that these surface residues play a role in recognition of other proteins in the Get pathway.

Changes in switch helices are normally coupled to functional changes. Although there was little conformational change in ArsA nucleotide structures it was postulated that binding of ATP would cause a conformational change in Switch II that would be transmitted to a His involved in metal coordination (22). This residue (*Sc*H172) is the only coordinating residue from ArsA that is found in Get3 and in our structure this is in a position to interact with a network of salt bridges that appear to stabilize the base of SB1/2 (Fig. S4*C*). Mutations of these residues had LOF phenotypes; however, they were not strong and it may be possible that coupling of Switch II changes is not essential for TA binding.

Get3 binds a variety of TA-protein substrates via hydrophobic interactions (4) and it is difficult to decide what mutations might interfere with binding. Based on the predicted pocket, we generated extensive mutations in SB1 and SB2. As expected, mutations in the predicted TA-protein binding pocket (I136S, D137A, L140S, S141A, M143S, and L219S) had LOF; however, the majority of the residues had no phenotype including those disordered in our structure (Fig. 4*B* and Fig. S4*D*). This hydrophobic interaction may require multiple mutations in the binding pocket to see significant disruptions.

The lack of conservation of the SB2 residue *Af*R200 made a comparable mutation in *Sc* impossible. Due to its location in the nucleotide-binding pocket in the *Af*Get3-ADP structure we decided to see if its mutation would have an effect on rescue by *Af*Get3. An *Af*R200A mutation was a clear LOF phenotype (Figs. 2*A* and 4*A*). This is in contrast to a number of other mutations, including some disordered residues, in this region of SB2 that showed no phenotypes. It is difficult to envision an effect of the *Af*R200A mutation in the absence of the hexamer.

A mutation of the conserved deviant P-loop lysine is expected to completely abolish function and should be a strong phenotype. In the *Af*Get3-ADP structure this residue makes no contacts (Fig. 4 and Fig. S4*A*), still, a mutation of this residue to Ala (*Sc*K26A) was the strongest phenotype of all. In the Ras/RasGAP case any mutation of the Arg-finger leads to a total LOF even the seemingly benign mutation to Lys (31). We did the same type of mutation, *Sc*K26R, and found that this mutant is a strong LOF phenotype, although not as strong as *Sc*K26A.

Discussion

Get3 must couple ATP hydrolysis to TA-protein binding and release. To propose a mechanism for Get3 binding of TA-proteins we can model the transition to a closed-bound state

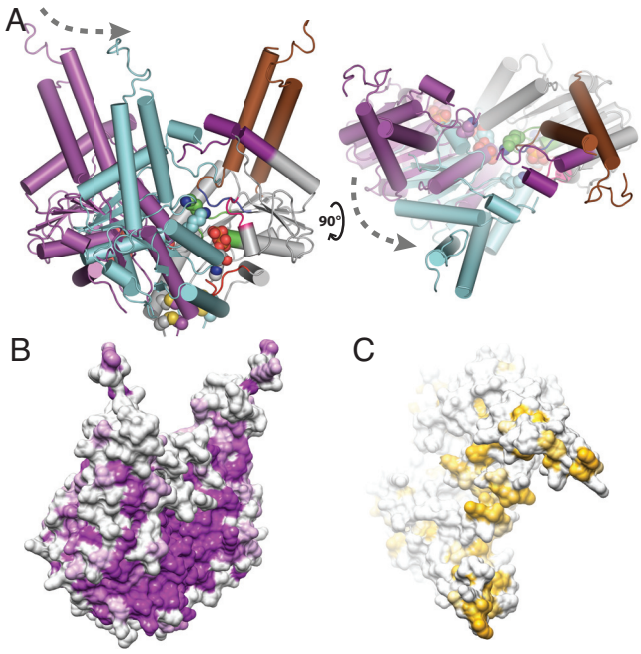

Fig. 5. NifH-like model. (*A*) An overlay of *Af*Get3-ADP in the open dimer and the closed NifH(1m34)-like model. The *Af*Get3-ADP dimer, similar to Fig. 1*B*, is colored with the right monomer by feature and the left in purple. The modeled rotated monomer is in light blue. *Af*K34 and the bridged cysteines shown as spheres. Arrows indicate direction of motion. (*B*) Conserved surface of the NifH-like model oriented as left *A*. (*C*) Hydrophobic surface of the NifH-like model orientated as right *A*.

based on the NifH structures. We believe our structures represent various open, non-substrate binding conformations where the hydrophobic SB1/2 are highly flexible and open for interaction with proteins, possibly in a metastable hexameric state. The binding of ATP couples to a re-arrangement of the Switch loops that would be transmitted to SB1/2. Binding would also involve a rotation and translation at the dimer interface that moved the bridging *Sc*K26 (*Af*34) into a position to counter the additional charge of the γ-phosphate (modeled in Fig. 5*A*). The *Af*Get3-apo dimer shows how some of this motion could occur as it rotates inward, relative to the *Af*Get3-ADP dimer, demonstrating flexibility at this interface (Fig. S2*E*). There are clashes in this simple NifH-like model and we believe that additional conformational changes must occur.

This ATP bound complex would bury a considerable amount of the conserved residues at the dimer interface (Fig. 5*B*) and would bring SB1/2 from opposing dimers into a closer orientation, creating a large hydrophobic groove at the top of the interface (Fig. 5*C*). This structure would be incompatible with our hexamer but would provide a favorable binding surface for a TA-protein. The TM helix would dock in the groove formed at the base of SB2 and the hydrophobic flexible loop of SB1 could then wrap around it, similar to SRP signal sequence finger-loop binding (32). The only component missing in such a model is the residue that would activate the catalytic water. It is possible that additional partner binding at the membrane would either donate this group or lead to additional conformational changes in Get3 that would stimulate ATP hydrolysis once the substrate has been delivered.

The oligomeric state of Get3 based on this work leads to open questions about function. By homology to NifH and ArsA, we have described a model in which the NHD dimer interactions are the most relevant to TA-protein binding; however, we find it difficult to ignore the arm dimer interface. In all of our crystal

structures, SB1/2 interactions bury a significant amount of hydrophobic surface implying that they have a high affinity for binding protein (Fig. 1*D* and Fig. S2 *C* and *F*). In an open form these surfaces should be very unstable and it is hard to imagine that they could exist free in the cytoplasm. The hexamer seen in our crystal structure could be a stable resting form of the protein that needs additional factors, such as the Get4/Get5 proteins (7), to transition to the open dimer state. Another possibility is that the hexamer operates as an ADP-exchange factor (like a GEF for Ras) stabilizing the apo form for ATP binding by displacing the Mg^{2+} and releasing ADP. In *Af*Get3 the R200 salt bridges to the ADP β-phosphate, which would seem to stabilize the ADP form; however, the concentration of ADP in our crystal conditions is very high and the binding could be an artifact of that. A third, less likely, possibility would be that the hexamer is the active form of the complex and that TA proteins are stabilized in the flexible hydrophobic center reminiscent of some AAA ATPases (33). Evidence that supports a role for the hexamer is the importance of *Af*R200, a purified human Get complex sediments at a compatible size (4), the functional form of ArsA is a multimer (34), and a trimeric form of ArsA has been visualized by EM and chromatography (35).

Proper synthesis and targeting of TA-proteins by the Get pathway have broad implications in biology, as they are essential in many cellular homeostasis and transport processes. Our structural and functional studies are a mechanistic look at the recently identified pathway component Get3. These experiments allow us to define a model that predicts the conformational changes in Get3 that are involved in TA-protein and nucleotide binding (Fig. S5). They also suggest an oligomeric form that may play a key role. Many aspects of TA-protein targeting, such as the specifics of substrate binding, interactions of partners and the kinetic steps of recognition and release, remain to be determined.

Methods

Full methods are provided in the *SI Text* including a crystallographic table and a full list of the mutants tested. We briefly discuss the methods here. C-terminally 6×His tagged *A. fumigatus* and *S. cerevisiae* Get3 coding sequences were cloned into pET33b vectors. Get3 was expressed in *E. coli* cells and purified with Ni-affinity and size exclusion chromatography. Initial crystallization conditions were identified in standard screens. *Af*Get3-ADP experimental phases were obtained from seleno-methionine derivatives using multiple-wavelength anomalous dispersion. Phases for both apo forms were obtained by molecular replacement. For growth assays, *Af* and *Sc*Get3 coding sequences were cloned into YEp352 vector and mutations were made with site-directed mutagenesis. Constructs were transformed into the strains BY4741 and the Get3 knockout strain BY4741 *YDL100c*::*kanMX4*.

ACKNOWLEDGMENTS. We thank S. Shan and A. Palazzo for discussion and critical comments on the manuscript and Gordon and Betty Moore for support of the Molecular Observatory at Caltech. All data collection was performed at beamline 12-2 at Stanford Synchrotron Radiation Lightsource and we thank G. Card and M. Soltis for beamline assistance. Operations at SSRL are supported by the U.S. Department of Energy and National Institutes of Health. W.M.C. is supported by the Searle Scholar program and a Burroughs-Wellcome Fund Career Award for the Biological Sciences.

1. Kutay U, Hartmann E, Rapoport TA (1993) A class of membrane proteins with a C-terminal anchor. *Trends Cell Biol* 3:72–75.
2. Borgese N, Brambillasca S, Colombo S (2007) How tails guide tail-anchored proteins to their destinations. *Curr Opin Cell Biol* 19:368–375.
3. Schuldiner M, et al. (2005) Exploration of the function and organization of the yeast early secretory pathway through an epistatic miniarray profile. *Cell* 123:507–519.
4. Stefanovic S, Hegde RS (2007) Identification of a targeting factor for post-translational membrane protein insertion into the ER. *Cell* 128:1147–1159.
5. Schuldiner M, et al. (2008) The GET complex mediates insertion of tail-anchored proteins into the ER membrane. *Cell* 134:634–645.
6. Favaloro V, Spasic M, Schwappach B, Dobberstein B (2008) Distinct targeting pathways for the membrane insertion of tail-anchored (TA) proteins. *J Cell Sci* 121:1832–1840.
7. Jonikas M, et al. (2009) Comprehensive characterization of genes required for protein folding in the endoplasmic reticulum. *Science* 323:1693–1697.
8. Boskovic J, et al. (1996) The sequence of a 16,691-bp segment of *Saccharomyces cerevisiae* chromosome IV identifies the DUN1, PMT1, PMT5, SRP14, and DPR1 genes, and five new open reading frames. *Yeast* 12:1377–1384.
9. Shen J, Hsu CM, Kang BK, Rosen BP, Bhattacharjee H (2003) The *Saccharomyces cerevisiae* Arr4p is involved in metal and heat tolerance. *Biometals* 16:369–378.
10. Tseng Y, Yu C, Liao V (2007) *Caenorhabditis elegans* expresses a functional ArsA. *FEBS J* 274:2566–2572.
11. Kao G, et al. (2007) ASNA-1 positively regulates insulin secretion in *C. elegans* and mammalian cells. *Cell* 128:577–587.
12. Hemmingsson O, Zhang Y, Still M, Naredi P (2009) ASNA1, an ATPase targeting tail-anchored proteins, regulates melanoma cell growth and sensitivity to cisplatin and arsenite. *Cancer Chemother Pharmacol* 63:491–499.
13. Hann BC, Walter P (1991) The signal recognition particle in *S. cerevisiae*. *Cell* 67:131–144.
14. Zúñiga S, Boskovic J, Jiménez A, Ballesta JP, Remacha M (1999) Disruption of six *Saccharomyces cerevisiae* novel genes and phenotypic analysis of the deletants. *Yeast* 15:945–953.
15. Sprang SR (1997) G protein mechanisms: Insights from structural analysis. *Annu Rev Biochem* 66:639–678.
16. Koonin EV (1993) A superfamily of ATPases with diverse functions containing either classical or deviant ATP-binding motif. *J Mol Biol* 229:1165–1174.
17. Netz D, Pierik A, Stümpfig M, Mühlenhoff U, Lill R (2007) The Cfd1-Nbp35 complex acts as a scaffold for iron-sulfur protein assembly in the yeast cytosol. *Nat Chem Biol* 3:278–286.
18. Schindelin H, Kisker C, Schlessman JL, Howard JB, Rees DC (1997) Structure of ADP·AlF$_4$(-)-stabilized nitrogenase complex and its implications for signal transduction. *Nature* 387:370–376.
19. Schlessman JL, Woo D, Joshua-Tor L, Howard JB, Rees DC (1998) Conformational variability in structures of the nitrogenase iron proteins from *Azotobacter vinelandii* and *Clostridium pasteurianum*. *J Mol Biol* 280:669–685.
20. Milburn MV, et al. (1990) Molecular switch for signal transduction: Structural differences between active and inactive forms of protooncogenic ras proteins. *Science* 247:939–945.
21. Scheffzek K, et al. (1997) The Ras-RasGAP complex: Structural basis for GTPase activation and its loss in oncogenic Ras mutants. *Science* 277:333–338.
22. Zhou T, Radaev S, Rosen BP, Gatti DL (2001) Conformational changes in four regions of the *Escherichia coli* ArsA ATPase link ATP hydrolysis to ion translocation. *J Biol Chem* 276:30414–30422.
23. Lutkenhaus J, Sundaramoorthy M (2003) MinD and role of the deviant Walker A motif, dimerization and membrane binding in oscillation. *Mol Microbiol* 48:295–303.
24. Andreeva A, et al. (2008) Data growth and its impact on the SCOP database: New developments. *Nucleic Acids Res* 36:D419–425.
25. Zhou T, Radaev S, Rosen BP, Gatti DL (2000) Structure of the ArsA ATPase: The catalytic subunit of a heavy metal resistance pump. *EMBO J* 19:4838–4845.
26. Freymann DM, Keenan RJ, Stroud RM, Walter P (1997) Structure of the conserved GTPase domain of the signal recognition particle. *Nature* 385:361–364.
27. Montoya G, Svensson C, Luirink J, Sinning I (1997) Crystal structure of the NG domain from the signal-recognition particle receptor FtsY. *Nature* 385:365–368.
28. Georgiadis MM, et al. (1992) Crystallographic structure of the nitrogenase iron protein from *Azotobacter vinelandii*. *Science* 257:1653–1659.
29. Krissinel E, Henrick K (2007) Inference of macromolecular assemblies from crystalline state. *J Mol Biol* 372:774–797.
30. Metz J, Wächter A, Schmidt B, Bujnicki JM, Schwappach B (2006) The yeast Arr4p ATPase binds the chloride transporter Gef1p when copper is available in the cytosol. *J Biol Chem* 281:410–417.
31. Ahmadian MR, Stege P, Scheffzek K, Wittinghofer A (1997) Confirmation of the arginine-finger hypothesis for the GAP-stimulated GTP-hydrolysis reaction of Ras. *Nat Struct Biol* 4:686–689.
32. Schaffitzel C, et al. (2006) Structure of the *E. coli* signal recognition particle bound to a translating ribosome. *Nature* 444:503–506.
33. Ogura T, Wilkinson AJ (2001) AAA+ superfamily ATPases: Common structure diverse function. *Genes Cells* 6:575–597.
34. Hsu CM, Kaur P, Karkaria CE, Steiner RF, Rosen BP (1991) Substrate-induced dimerization of the ArsA protein, the catalytic component of an anion-translocating ATPase. *J Biol Chem* 266:2327–2332.
35. Wang HW, et al. (2000) Trimeric ring-like structure of ArsA ATPase. *FEBS Lett* 469:105–110.